Differentiation of human embryonic stem cells on three-dimensional polymer scaffolds

Shulamit Levenberg*, Ngan F. Huang*, Erin Lavik†, Arlin B. Rogers‡, Joseph Itskovitz-Eldor§, and Robert Langer*¶

*Department of Chemical Engineering, Divisions of †Health Sciences and Technology, and ‡Comparative Medicine, Massachusetts Institute of Technology, Cambridge, MA 02139; and §Department of Obstetrics and Gynecology, Rambam Medical Center, Faculty of Medicine, The Technion, 35245 Haifa, Israel

Contributed by Robert Langer, August 25, 2003

Human embryonic stem (hES) cells hold promise as an unlimited source of cells for transplantation therapies. However, control of their proliferation and differentiation into complex, viable 3D tissues is challenging. Here we examine the use of biodegradable polymer scaffolds for promoting hES cell growth and differentiation and formation of 3D structures. We show that complex structures with features of various committed embryonic tissues can be generated, *in vitro*, by using early differentiating hES cells and further inducing their differentiation in a supportive 3D environment such as poly(lactic-*co*-glycolic acid)/poly(L-lactic acid) polymer scaffolds. We found that hES cell differentiation and organization can be influenced by the scaffold and directed by growth factors such as retinoic acid, transforming growth factor β, activin-A, or insulin-like growth factor. These growth factors induced differentiation into 3D structures with characteristics of developing neural tissues, cartilage, or liver, respectively. In addition, formation of a 3D vessel-like network was observed. When transplanted into severe combined immunodeficient mice, the constructs continue to express specific human proteins in defined differentiated structures and appear to recruit and anastamose with the host vasculature. This approach provides a unique culture system for addressing questions in cell and developmental biology, and provides a potential mechanism for creating viable human tissue structures for therapeutic applications.

Embryonic stem (ES) cells, including human ES (hES) cells, represent a promising source for cell transplantation because of their unique ability to give rise to all somatic cell lineages (1–3). ES cell differentiation can be induced in monolayer culture (4, 5) or by removing the cells from their feeder layer and growing them in suspension where they form embryoid bodies (EBs) (6–8). Chemical cues provided directly by growth factors or indirectly by feeder cells can induce ES cell differentiation toward specific lineages (4, 9–11). However, it has been difficult to control cell proliferation and differentiation into higher-order structures, which might be directly used for tissue engineering applications.

We hypothesized that porous biodegradable polymer scaffolds can be used to support ES cells because they represent a promising system for allowing formation of complex 3D tissues during differentiation. The scaffold provides physical cues for cell orientation and spreading, and pores provide space for remodeling of tissue structures (12). In addition, directed degradation of scaffolds can be used as a tool for localized and controlled growth factor supplementation (13). Ultimately, *in vitro*-differentiated constructs can potentially be used for transplantation.

Therefore, the goal of this study was to engineer tissue-like constructs derived from hES cells by using polymer scaffolds. We hypothesized that combining the appropriate physical support (provided by the biodegradable polymer scaffolds) with chemical cues could possibly create a supportive environment to direct differentiation and organization of hES cells. To test this, we created a series of 3D culture conditions using biodegradable scaffolds and matrigel. Here we show that polymer scaffolds, designed to resist contraction under the compressive stress exerted by the cells, promoted proliferation, differentiation, and organization of hES cells into 3D structures. Furthermore, variation of growth factor conditions induced formation of human 3D structures with characteristics of developing cartilage, liver, neural tissues, and blood vessels. When transplanted into severe combined immunodeficient (SCID) mice, the constructs maintain their viability and continue to express specific human proteins in defined differentiated structures. Moreover, the implants appear to recruit and anastamose with the host vasculature.

Materials and Methods

Cell Culture. hES cells (H9 clone) were grown on mouse embryonic fibroblasts (Cell Essential, Boston) in knockout medium as described (6). To induce formation of EBs, hES cell colonies were dissociated with 1 mg/ml collagenase type IV and suspended in differentiation media without lymphocyte inhibitory factor (LIF) and basic fibroblast growth factor in Petri dishes (6).

Scaffold Preparation. The scaffolds consisted of a 50/50 blend of poly(lactic-*co*-glycolic acid) (PLGA) (Boehringer Ingelheim Resomer 503H, Ingelheim, Germany, $M_n \approx 25{,}000$) and poly(L-lactic acid) (PLLA) (Polysciences, Warrington, PA, $M_n \approx 300{,}000$). The sponges were fabricated by a salt-leaching process as described (14). For cell differentiation experiments, the sponges were cut into rectangular pieces of $\approx 5 \times 4 \times 1$ mm^3. Before cell seeding, they were sterilized overnight in 70% (vol/vol) ethanol and washed three times in PBS.

Cell Differentiation on Matrigel and Scaffolds. For seeding in matrigel, 8- to 9-day-old EBs were trypsinized, and 0.8×10^6 cells were mixed in 25 μl of a 50% (vol/vol) medium and matrigel (growth factor-reduced, BD Biosciences, Bedford, MA). EB medium was supplemented with the following growth factors: transforming growth factor (TGF)-β1 (2 ng/ml), activin-A (20 ng/ml), and insulin-like growth factor (IGF) I (10 ng/ml) (R & D Systems), and retinoic acid (RA) (300 ng/ml) (Sigma). The mixture solidified in a six-well Petri dish at 37°C incubator and then detached from the dish with sterile blades. Four milliliters of each respective EB medium was added. For seeding on scaffolds, 0.8×10^6 cells (from undifferentiated hES or EBs at day 8) were seeded into each scaffold by using 25 μl of a mixture containing 50% (vol/vol) of matrigel and the respective EB medium. After seeding the cells, scaffolds were suspended in six-well Petri dishes in their respective medium. For some experiments, scaffolds were soaked in 50 μg/ml fibronectin (Sigma) for 1 h and washed in PBS before direct cell seeding (without matrigel) in 25 μl of EB medium.

Abbreviations: ES, embryonic stem; hES, human ES; EB, embryoid body; RA, retinoic acid; H&E, hematoxylin and eosin; AFP, α-feto-protein; TGF, transforming growth factor; IGF, insulin-like growth factor; PLLA, poly(L-lactic acid); PLGA, poly(lactic-*co*-glycolic acid); SCID, severe combined immunodeficient.

¶To whom correspondence should be addressed. E-mail: rlanger@mit.edu.

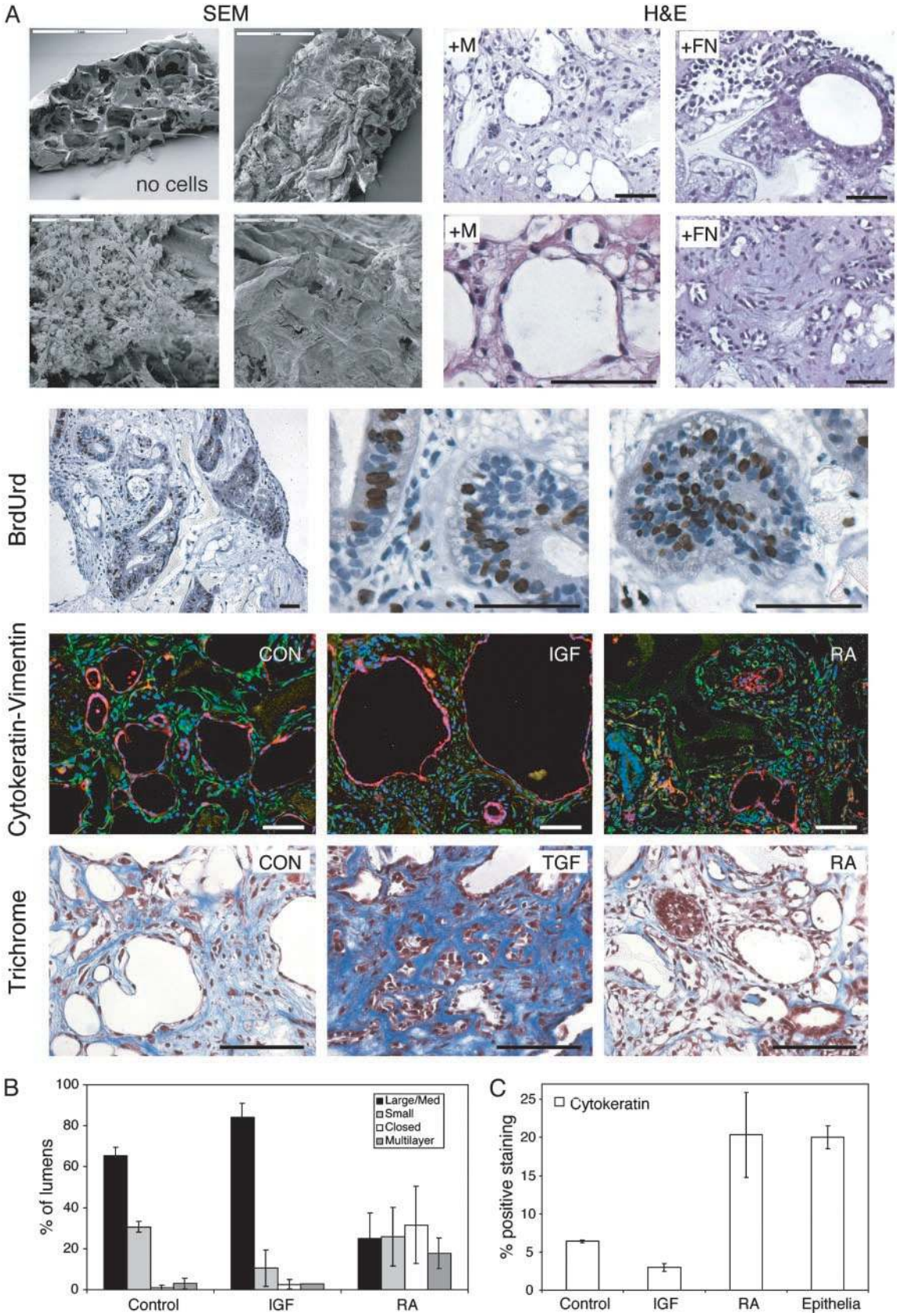

Fig. 1. Scaffolds support hES cell attachment, proliferation, and differentiation into 3D tissue-like structures. (*A*) Scanning electron microscopy (SEM) of PLLA/PLGA scaffolds without and with differentiating hES cells, showing the attachment of the cells to the scaffolds in different magnifications. (Scale bars: *Upper*, 1 mm; *Lower Left*, 50 μm; *Right*, 200 μm.) For histological examination with H&E stain, hES cells were seeded onto the scaffold by using two methods of cell attachment: seeding the cells onto the scaffold with matrigel (+M) or coating the scaffold with fibronectin (+FN). For analysis of cell proliferation in the constructs (BrdUrd), constructs were incubated with BrdUrd and stained with anti-BrdUrd antibodies (brown) after 2 weeks of culture. Low and high

Tissue Processing and Immunohistochemical Staining. Tissue constructs were fixed for 6 h in 10% neutral buffered formalin, routinely processed, and embedded in paraffin. Five-micrometer-thick transverse sections were placed on silanized slides for immunohistochemistry or staining with hematoxylin and eosin (H&E), trichrome, or safranin-O. Immunohistochemical staining was carried out by using the Biocare Medical Universal HRP-DAB kit (Biocare Medical, Walnut Creek, CA) according to the manufacturer's instructions, with prior heat treatment at 90°C for 20 min in ReVeal buffer (Biocare Medical) for epitope recovery. The primary antibodies were anti-human α-feto-protein (AFP) (1:2,500), cytokeratin-7 (1:25), CD31 (1:20), albumin (1:100), vimentin (1:50), S100 (1:100), Desmin (1:150), Myogenin (1:150), and Insulin (1:100) (all from Dako). Anti-human β_{III}-tubulin (Sigma, 1:500), nestin (Transduction Laboratories, 1:1,000), CD34 (Labvision, Fremont, CA, 1:20), SSEA4 (Hybridoma bank, University of Iowa, Ames, 1:4), and Tra 1–60 (a gift from Peter Andrews, University of Sheffield, Sheffield, U.K., 1:10). Human and mouse tissues (Dako) were used as controls to ensure antibody specificity (see Fig. 6, which is published as supporting information on the PNAS web site, www.pnas.org). For proliferation studies, culture medium was incubated with 10 μm of BrdUrd (Sigma) for 3 h before fixation. Tissue sections were stained by using mouse anti-BrdUrd antibodies (1:1,000).

RT-PCR analysis. Total RNA was isolated by an RNEasy Mini kit (Qiagen, Valencia, CA). RT-PCR was carried out by using a Qiagen OneStep RT-PCR kit with 10 units of RNase inhibitor (GIBCO) and 40 ng of RNA. Primer sequences, reaction conditions, and cycle numbers were as described (9, 14). The amplified products were separated on 1.2% agarose gels with ethidium bromide (E-Gel, Invitrogen).

Mechanical Testing. For tensile testing of the sponge alone, sponges were trimmed to dimensions 0.4 mm by 5 mm by 11 mm, and tested at a strain rate of 0.05 mm/s until failure by using an Instron 5542 apparatus (Instron, Canton, MA). Compression testing was performed on sponges alone and sponges with matrigel in a parallel plate load cell by using the instron 5542 apparatus. The sponges were porous discs of 17 mm in diameter with a thickness of 0.8 mm. Samples were first precycled one time by using a 5% strain at a strain rate of 0.1 mm/mm per s before testing at the same strain rate.

Transplantation into SCID Mice. Grown on scaffolds for 2 weeks *in vitro*, differentiating hES cells were implanted s.c. in the dorsal region of 4-week-old SCID mice (CB.17.SCID, Taconic Farms). Scaffolds implanted without cells were used as controls. Fourteen days after transplantation, the implants were retrieved, fixed overnight in 10% buffered formalin at 4°C, embedded in paraffin, and sectioned for histological examination.

Results and Discussion

To create a 3D supportive environment for directing differentiation and organization of hES cells into tissue-like structures, we used biodegradble scaffolds. Polymer scaffolds were fabricated from a blend of 50% PLGA and 50% PLLA. The PLGA was selected to degrade quickly ($\approx$3 weeks) to facilitate cellular ingrowth, whereas the PLLA was chosen to provide mechanical stiffness to support 3D structures. The pore size of 250–500 μm was chosen to facilitate the seeding and ingrowth of cells. We evaluated attachment and 2-week survival of differentiating hES cells (EB day 8 cells) seeded into the scaffolds by using two methods of seeding: (*i*) seeding the cells onto the scaffold with matrigel, or (*ii*) coating the scaffold with fibronectin. Both methods facilitated cell attachment, growth, and viability. The cells lined the inner and outer surfaces of the scaffold, filling the pores, as demonstrated by scanning electron microscopy and histology (Fig. 1*A*). After the 2-week period, immunohistochemical staining of BrdUrd incorporation confirmed high levels of cellular proliferation (Fig. 1*A*). We used differentiating hES cells, rather than undifferentiated hES cells, based on observations that scaffolds seeded with undifferentiated hES cells exhibited clear perforation of the outer surfaces and less uniform growth and survival in the center of the scaffolds when compared with differentiating hES cells (EB day 8) (Fig. 7, which is published as supporting information on the PNAS web site).

After the incubation period, the constructs exhibited 3D organization resembling primitive tissue structures. We assessed the morphologic and biochemical phenotype of differentiating hES cell-derived 3D structures grown on polymer scaffolds and supplemented with representative growth factors known to induce ES cell differentiation: RA, activin-A, TGF-β, or IGF-I (Fig. 1). IGF supplementation resulted in formation of relatively large open tubular structures lined by a single layer of cytokeratin-positive cuboidal-to-columnar epithelial cells, whereas RA induced formation of smaller circular multilayered bodies with narrow or unapparent lumens (Fig. 1 *A* and *B*). RA supplementation resulted in an $\approx$4-fold increase in the total percentage of cytokeratin-positive areas, comparing to control samples, approaching a level found in adult lung (Fig. 1*C*). The cellular structures secreted extracellular matrix components. Collagen production, demonstrated by trichrome stain, and cell-matrix organization were dramatically influenced by growth factor supplements (Fig. 1*A*).

Addition of TGF-β to the medium induced formation of tissue that secreted a cartilage-like glycosaminoglycan extracellular matrix (15), as demonstrated by safranin-O staining (Fig. 2). In contrast, addition of other growth factors, even in combination with TGF-β, resulted in no safranin-O-positive matrix deposition (Fig. 2). RT-PCR analysis indicated higher levels of cartilage matrix protein (CMP) gene expression in constructs conditioned with TGF-β, compared with other samples (Fig. 3).

Addition of activin-A or IGF induced the formation of structures with biochemical features found in developing liver (16). Compared with unconditioned controls, activin-A-treated constructs produced high levels of AFP and albumin throughout the sample. IGF induced high levels of AFP and albumin in more defined areas (Fig. 2), whereas no staining was observed with the addition of RA. These results suggest that, in scaffold-supported

magnifications show proliferating cells throughout the sample. [Scale bars (H&E, BrdUrd) = 50 μm.] For expression and organization of cytokeratin and vimentin as epithelial and mesenchymal markers in tissue constructs, constructs grown for 2 weeks in control medium (CON) or in the presence of IGF or RA were sectioned and stained with anti-cytokeratin antibodies (red), anti-vimentin antibodies (green), and DAPI for nuclear staining (blue). Cytokeratin-positive cells form tubulocystic structures with open lumens. To show extracellular collagen formation (trichrome staining) induced by TGF-β, construct sections were stained with Masson's trichrome for collagen (blue). [Scale bars (cytokeratin, trichrome) = 100 μm.] (*B*) Comparison of lumen diameters of tubular structures lined by cytokeratin-positive epithelium. Cytokeratin-positive tubular structures were counted, and lumen diameters were measured and grouped according to size [large >200 μm, medium (Med) >40 μm, small <40 μm], closed, and multilayered lumens. The results are shown as percentages of lumens in each group from total number of lumens in each sample. The results shown are mean values ($\pm$SD) of samples obtained in two different experiments performed in duplicate. (*C*) Quantitative analysis of cytokeratin staining. Percentage of positive staining corresponds to percentages of area positively stained with the antibody within the tissue sections. The results shown are mean values ($\pm$SD) of sample sections obtained in two different experiments performed in duplicate and sections of normal human lung tissue (Epithelia).

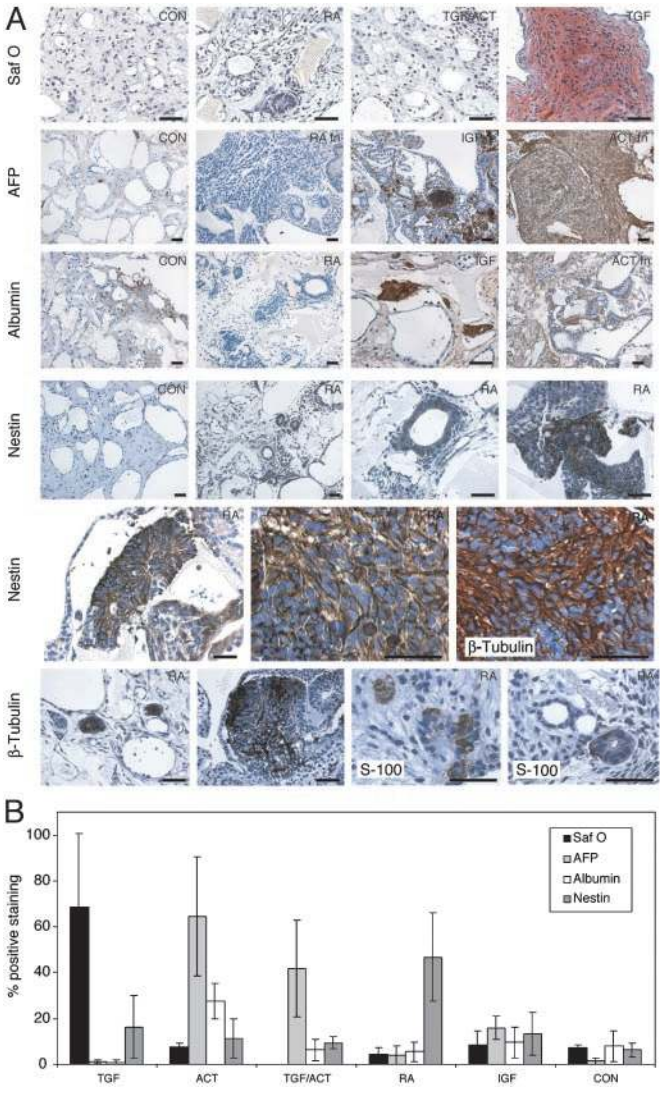

Fig. 2. Differentiation into mesodermal-, ectodermal-, and endodermal-derived cell types and tissue-like structures. (*A*) Immunostaining of tissue sections taken from hES constructs incubated for 2 weeks with control medium (CON) or medium supplemented with growth factors: TGF-β (TGF), activin-A (ACT), RA, IGF, and a combination of TGF-β and activin-A (TGF/ACT). Samples were stained with safranin-O (Saf O) or with antibodies against human AFP, albumin, nestin, β_{III}-tubulin, and S-100. (Scale bars = 50 μm.) (*B*) Quantitative analysis of antibody staining. Percentage of positive staining corresponds to percentages of area positively stained with the antibody within the tissue sections. The results shown are mean values ($\pm$SD) of sample sections obtained in three different experiments performed in duplicate.

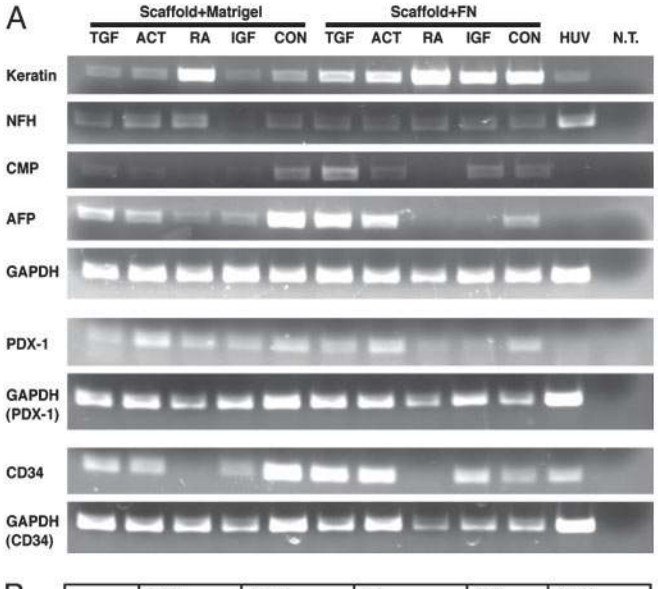

B

	TGF		ACT		RA		IGF		CON	
	M	F	M	F	M	F	M	F	M	F
Keratin	+	++	+	++	+++	++++	+	++	+	+++
NFH	++	+	++	+	++++	++	-	++	+	++
CMP	+++	++++	+	+	+	+	+	++	+++	++
AFP	++	+++	++	+++	+	-	+	-	+++	++
PDX-1	++	++	++++	++++	++	+	++	+	+++	++++
CD34	++	+++	++	+++			++	+++	+++	++

M= Matrigel F= FN

Fig. 3. Expression of genes in 3D constructs treated with various growth factors. (*A*) RNA was isolated from constructs grown for 2 weeks in the presence of TGF-β (TGF), activin-A (ACT), RA, IGF, and control medium (CON), and subjected to RT-PCR analysis using primers for the following genes: ultra-high sulfur keratin (keratin), neurofilament heavy chain (NFH), cartilage matrix protein (CMP), AFP, PDX-1, CD34, and GAPDH. No template (N.T.) was used as a control. (*B*) Schematic representation of the growth factor effects based on semiquantitative analysis of gene expression. For each gene, mean pixel intensities of each band were measured and normalized to mean pixel intensities of GAPDH band. Based on normalized pixel intensities, the results were presented in a summary table and ranged from + (low expression) to ++++ (highest expression).

hES 3D constructs, activin-A and IGF can induce endodermal differentiation into liver-like cells. Gene expression analysis indicated higher levels of the pancreatic gene PDX-1 in tissue-constructs treated with activin-A compared with other growth factors (Fig. 3), which may support the role of activin-A in inducing differentiation of hES cells into endodermal-derived tissues on polymer scaffolds.

RA supplementation resulted in development of stratified and pseudostratified epithelial-lined solid, rosette-like, and ductular structures (Figs. 1*A* and 2). Rosettes were morphologically similar to those seen in the embryonic neural tube and were positive for nestin and β_{III}-tubulin, as were many non-rosette-like structures in RA-conditioned constructs (Fig. 2). S-100, a protein associated with neuroectodermal derivation, was present in cells surrounding some tubes (Fig. 2). Gene expression analysis of samples treated with RA indicated high levels of keratin and neurofilament RNA and very low expression of mesodermal and endodermal genes, in contrast to other samples (Fig. 3). These results suggest that RA can preferentially induce ectodermal differentiation and formation of 3D neuroectodermal-like structures in hES cells grown on polymer scaffolds.

Because a vascular supply is crucial to the formation of higher-order tissue structures (17), we analyzed whether polymer scaffold-supported hES cells were able to differentiate and organize into vessels. Histological evaluation and immunohistochemical staining for CD34 and CD31 demonstrated the presence of capillary-like networks displaying endothelial cell-associated surface molecules throughout the tissue construct (Fig. 4). Comparison of vessel-like structures in the scaffolds in the presence and absence of matrigel indicated that matrigel was not required, as samples seeded on fibronectin-coated scaffolds (without matrigel) resulted in higher levels of endothelial differentiation and vascularization. The differences might be caused by effects of fibronectin or growth factors still present in the matrigel after growth factor reduction. Unlike other constructs, samples treated with RA neither formed CD34/CD31$^+$ capillary networks nor expressed CD34 or CD31 genes as shown by RNA analysis (Figs. 3 and 4). Elongated smooth muscle-like

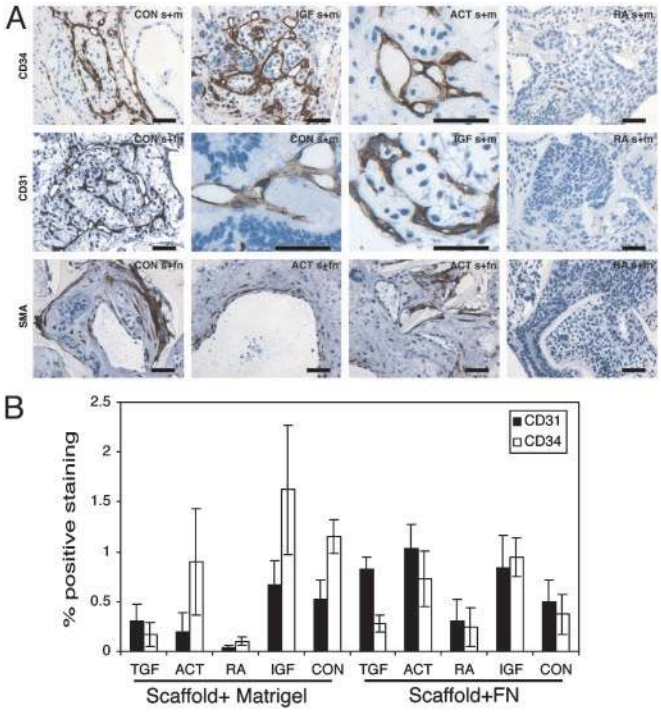

Fig. 4. Vessel-like network formation, *in vitro*, in hES 3D constructs. (*A*) Differentiating hES cells (EB day 8) were seeded on PLLA/PLGA scaffolds by using two methods of cell attachment: seeding the cells onto the scaffold with matrigel (scaffold plus matrigel, s+m) or coating the scaffold with fibronectin (scaffold plus FN, s+fn). The constructs were incubated in a control medium (CON) or medium supplemented with TGF-β (TGF), activin-A (ACT), RA, or IGF. After 2 weeks of incubation, the samples were fixed, sectioned, and immunostained by using anti-CD31, anti-CD34, or anti-smooth muscle actin (SMA) antibodies. (Scale bar = 50 μm.) Note the complex network formation in control and IGF-treated samples in contrast to the absence of staining in RA-treated samples. (*B*) Quantitative analysis of antibody staining. Percentage of positive staining corresponds to area of antibody-positive cells within the tissue sections. The results shown are mean values (±SD) of five different sample sections.

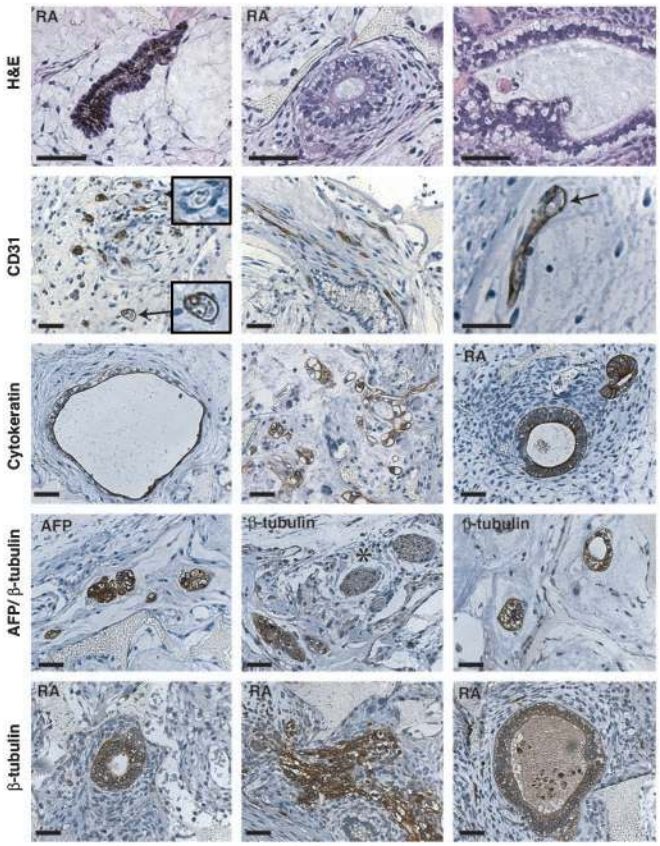

Fig. 5. Transplantation of hES-scaffold constructs into SCID mice. Two-week-old constructs (treated with RA or control medium) were implanted s.c. in the dorsal region of SCID mice. Fourteen-day-old implants were stained with H&E or with antibodies against human CD31, cytokeratin, AFP, or β_{III}-tubulin. Human-specific CD31 staining demonstrated the presence of both immunoreactive (construct-origin, arrows) and nonimmunoreactive (host origin, arrowhead) vessels. In certain instances there appeared to be continued differentiation and organization of constructs postimplantation. After continued construct maturation *in vivo*, RA-conditioned constructs exhibited larger and better organized neural structures than those seen *in vitro* (or with control medium *in vitro* or *in vivo*) including ductular structures lined by tall columnar epithelium invested with long cilia resembling ependymal cells, and rosettes with abundant melanin granules (brown/black in H&E section; confirmed by bleaching with potassium permanganate, data not shown). β_{III}-tubulin antibodies stained neuroectodermal structures within the implant as well as murine peripheral nerve fibers in surrounding connective tissue (asterisk). (Scale bar = 50 μm.)

cells were also detected, organized around some lumens, but not in samples treated with RA (Fig. 4).

To determine whether the scaffold had an effect on hES cell differentiation and 3D organization, we compared 2-week incubations of differentiating hES cells cultured on fibronectin-coated dishes versus fibronectin-coated scaffolds, as well as differentiation in matrigel alone versus matrigel with scaffold. The two-dimensional fibronectin-coated dish supported some cell differentiation (Fig. 8, which is published as supporting information on the PNAS web site) but could not support 3D structure formation. Matrigel alone could form a 3D environment, but it failed to support hES cell growth and 3D organization (Fig. 9, which is published as supporting information on the PNAS web site). One possibility is that the differences obtained between matrigel alone and scaffolds with matrigel could partially be caused by the scaffold's mechanical stiffness, which is necessary to resist the force of cell contraction. To determine whether the scaffold could withstand the types of mechanical forces exerted on the scaffold by proliferating and organizing cells, we carried out compressive and tensile tests (Fig. 9 *B–D*). Our results demonstrate that the polymer scaffold, with or without matrigel, exhibits a compressive modulus three orders of magnitude greater than that of matrigel alone (Fig. 9). This difference may be critical to higher-order organization by living cells. At the estimated cellular compressive stress of 110 Pa (see calculation in *Supporting Text*, which is published as supporting information on the PNAS web site) the scaffold, unlike matrigel alone, should contract by only 0.2%, providing a stable network for the development of pleiocellular 3D structures.

When comparing differentiation and organization of scaffold-grown constructs versus EBs, we found higher expression of differentiation-associated proteins such as cytokeratin, AFP, and nestin on the scaffolds, which correlated with more organization into defined epithelial tubular structures and neural tube-like rosettes (Fig. 10, which is published as supporting information on the PNAS web site). Regarding extracellular matrix production, no safranin-O staining was observed in EBs conditioned with TGF-β. The EB population was very heterogeneous in structure and protein expression levels. Consequently, polymer scaffolds appeared to be more suitable than EBs in promoting cell differentiation and homogeneity. The relatively small size of the EBs and high heterogeneity between EBs may limit their use in creating functional tissues for transplantation applications.

DEVELOPMENTAL BIOLOGY

To analyze the therapeutic potential of hES-derived polymer scaffold constructs, we surgically implanted 2-week-old constructs into s.c. tissue of SCID mice. At the time of implant retrieval (14 days after implantation), cells within constructs were viable and no signs of infection were detected. Implants were incompletely encapsulated by loose fibrogranulomatous connective tissue and permeated with host blood vessels. Immunohistochemical staining, using human-specific CD31 antibodies, demonstrated the presence of both immunoreactive (construct) and nonimmunoreactive (host) vessels throughout the constructs (Fig. 5). Moreover, construct-derived vessels contained intraluminal red blood cells, suggesting construct–host vascular anastamosis. Immunostaining with cytokeratin, β_{III}-tubulin, and AFP antibodies indicated that the implanted constructs continued to express these human proteins in defined structures within the scaffold area (Fig. 5). In certain instances there appeared to be continued differentiation and organization of constructs after implantation (Fig. 5), which was affected by the specific cytokine treatment before implantation. Staining with SSEA-4 and Tra 1–60 antibodies indicated that none of the cells remained undifferentiated (Fig. 11, which is published as supporting information on the PNAS web site).

Our results indicate that complex structures with features of various committed embryonic tissues can be generated, *in vitro*, by using early differentiating hES cells and further inducing their differentiation in a supportive 3D environment such as PLLA/PLGA polymer scaffolds. The *in vivo* results show that scaffold-supported hES constructs remain viable for at least 2 weeks, that constructs may recruit and anastamose with the host vascular system, and that the differentiation pattern induced *in vitro* remains intact or continues to progress *in vivo*. Growth of human tissues *in vitro* holds promise for addressing organ shortages and infectious disease risks, which present serious challenges in transplantation medicine. Further studies are required to promote tissue differentiation *in vitro* and *in vivo* and to address regulation of cellular proliferation to allay concerns regarding the potential tumorigenicity of undifferentiated and precursor cells (18, 19). In addition to potential clinical applications, *in vitro* tissue formation may provide an important tool for studying early human development and organogenesis. Future studies should include analysis of the long-term survival of the constructs *in vivo*, analysis of the functionality of the tissue structures formed, and further analysis of the chemical and physical cues and signals that induce 3D differentiation and organization on polymer scaffolds.

We thank Ernest Smith, Kathleen Cormier and Jeff Bajko for excellent assistance in tissue embedding and processing, Robert Marini for help with animal procedures, Mara Macdonald and Susan Matthews for help with staining and data analysis, and Justin S. Golub for help with RT-PCR assays. We also thank Keith Ligon for his advice and assistance with histology assessment. This work was supported by National Institutes of Health Grant HL60435.

1. Dushnik-Levinson, M. & Benvenisty, N. (1995) *Biol. Neonate* **67,** 77–83.
2. Thomson, J. A., Itskovitz-Eldor, J., Shapiro, S. S., Waknitz, M. A., Swiergiel, J. J., Marshall, V. S. & Jones, J. M. (1998) *Science* **282,** 1145–1147.
3. Wobus, A. M. (2001) *Mol. Aspects Med.* **22,** 149–164.
4. Kaufman, D. S., Hanson, E. T., Lewis, R. L., Auerbach, R. & Thomson, J. A. (2001) *Proc. Natl. Acad. Sci. USA* **98,** 10716–10721.
5. Reubinoff, B. E., Itsykson, P., Turetsky, T., Pera, M. F., Reinhartz, E., Itzik, A. & Ben-Hur, T. (2001) *Nat. Biotechnol.* **19,** 1134–1140.
6. Itskovitz-Eldor, J., Schuldiner, M., Karsenti, D., Eden, A., Yanuka, O., Amit, M., Soreq, H. & Benvenisty, N. (2000) *Mol. Med.* **6,** 88–95.
7. Shamblott, M. J., Axelman, J., Littlefield, J. W., Blumenthal, P. D., Huggins, G. R., Cui, Y., Cheng, L. & Gearhart, J. D. (2001) *Proc. Natl. Acad. Sci. USA* **98,** 113–118.
8. Carpenter, M. K., Inokuma, M. S., Denham, J., Mujtaba, T., Chiu, C. P. & Rao, M. S. (2001) *Exp. Neurol.* **172,** 383–397.
9. Schuldiner, M., Yanuka, O., Itskovitz-Eldor, J., Melton, D. A. & Benvenisty, N. (2000) *Proc. Natl. Acad. Sci. USA* **97,** 11307–11312.
10. Schuldiner, M., Eiges, R., Eden, A., Yanuka, O., Itskovitz-Eldor, J., Goldstein, R. S. & Benvenisty, N. (2001) *Brain Res.* **913,** 201–205.
11. Guan, K., Chang, H., Rolletschek, A. & Wobus, A. M. (2001) *Cell Tissue Res.* **305,** 171–176.
12. Vacanti, J. P. & Langer, R. (1999) *Lancet* **354,** Suppl. 1, SI32–SI34.
13. Richardson, T. P., Peters, M. C., Ennett, A. B. & Mooney, D. J. (2001) *Nat. Biotechnol.* **19,** 1029–1034.
14. Levenberg, S., Golub, J. S., Amit, M., Itskovitz-Eldor, J. & Langer, R. (2002) *Proc. Natl. Acad. Sci. USA* **99,** 4391–4396.
15. Naumann, A., Dennis, J. E., Awadallah, A., Carrino, D. A., Mansour, J. M., Kastenbauer, E. & Caplan, A. I. (2002) *J. Histochem. Cytochem.* **50,** 1049–1058.
16. Abe, K., Niwa, H., Iwase, K., Takiguchi, M., Mori, M., Abe, S. I. & Yamamura, K. I. (1996) *Exp. Cell Res.* **229,** 27–34.
17. Nomi, M., Atala, A., Coppi, P. D. & Soker, S. (2002) *Mol. Aspects Med.* **23,** 463–483.
18. Odorico, J. S., Kaufman, D. S. & Thomson, J. A. (2001) *Stem Cells* **19,** 193–204.
19. Donovan, P. J. & Gearhart, J. (2001) *Nature* **414,** 92–97.